Supporting Information

Vidal-Gadea et al. 10.1073/pnas.1108673108

SI Materials and Methods

Strains. The following strains were used: WT N2, *akEx387(Pdat-1::GFP; Pdat-1::ICE)*, *bas-1(ad446)*, *bas-1(ad446)*; *cat-4(ok342)*, *cat-2(e1112)*, *cat-4(ok342)*, *dop-1(vs101)*, *dop-1(vs100)*, *dop-2(vs105)*, *dop-2(tm1062)*, *dop-3(ok295)*, *dop-4(ok1321)*, *dop-4(tm1392)*, *dop-1(vs100) dop-3(vs106)*, *dop-1(vs100) dop-3(vs106)*; *dop-2(vs105)*, *dop-2(vs105)*; *dop-3(vs106)*, *egls-1(Pdat-1::GFP)*; *lgc-40(n4545)*, *mod-1(ok103)*, *otIs173(tph-1::GFP)*; *zdIs13(ttx-3 promo B::dsRed2) ser-1(ok345)*, *ser3(ok2007)*, *ser-3(ok1995)*, *ser-4(ok512)*, *ser-5(tm2654)*, *ser-5(ok3087)*, *ser-6(tm2146)*, *ser-6(tm2104)*, *ser-7(tm1325)*, *ser-1(ok345) ser-7(ok345)*, *tph-1(n4622)*, and *trp-4(sy695)*.

Statistical Analysis. For all comparisons in this study, $12 < n < 30$ with the single exception of body curvature amplitude, for which the number of frames manually checked (>1,000,000) necessitated sample sizes of $n = 5$ in our comparisons. All bars correspond to means, and variation is given as SEM throughout. All statistical analyses were performed using SigmaStat 3.5 (Aspire Software). Initial crawling, swimming, and postswim crawling were compared using one-way repeated-measures ANOVA (Holm-Sidak post hoc tests) when the data were parametric, and one-way repeated-measures ANOVA on ranks (Tukey post hoc tests) when the data were not. Comparisons between different experimental groups were performed by planned, two-tailed paired or unpaired *t* tests to compare different groups that were normally distributed. Differences between nonnormally distributed groups (or groups that failed the test of equal variance) were evaluated using the Mann-Whitney ranked sum test. In all cases, *P* values were reported using the convention: $^{*}P < 0.05$, $^{**}P < 0.001$.

Parameters Measured. ***Frequency.*** Measured as the frequency of bends that fully propagated along the body using the longest of either 20 cycles of uninterrupted forward locomotion or 1 min (for immobile-worms).
Amplitude. Defined as the angular excursion (degrees) of the second-most anterior of the 11 angles ("neck") describing body curvature (Fig. S1). For tail amplitudes we used the most posterior angle.
Velocity. Distance traveled in 1 min by body centroid in the direction of locomotion.
Swim onset. Time elapsed between water contact and the start of the first swim cycle.
Crawl onset. Time elapsed from the moment when the receding puddle formed a meniscus around the worm and when the worm crossed the initial puddle perimeter.
Swim performance. WT worms form a C-shaped posture at their ventral and dorsal apexes of their swim cycles (unlike the persistent S-shape during crawling; Fig. 1*A*). We quantified swim coordination as the number of swim cycles achieving C-shape over the total number of cycles in a 30-s window. We report averaged sets of 10 worms on three separate occasions.
Foraging while swimming. Animals tested above were also scored for foraging behavior while swimming. Mutant or ablated animals showing crawling bouts were scored as foraging only if they foraged while performing otherwise normal (C-shaped) swimming.

Pressure Assay. Three microliters of buffer was placed at the center of an agar-coated coverslip. Halocarbon oil was placed encircling the droplet to cushion a second coverslip while still allowing the nematode growth media (NGM) puddle to be compressed. Individual worms were transferred into the droplet. The second glass coverslip was placed on top of the preparation and allowed to gradually compress the puddle. Lastly, we inserted a flattened platinum wire between the two coverslips to pry the surfaces apart. The distance between the two glass surfaces was calculated using the known droplet volume and the area of the puddle obtained using ImagePro Plus (Media Cybernetics).

Magnetic Assay. Worms were fed iron particles mixed with *Escherichia coli* (OP50) for 1 h as previously described (1). Animals were transferred into NGM buffer on an agar-coated coverslip and placed on top of a custom-built electromagnet powered by a 12-V car battery. Worms were filmed for 1 min before, during, and after electromagnet activation.

Viscosity Assay. Methylcellulose (Sigma) solutions were prepared in NGM buffer as described by Korta et al. (2). Individual worms were filmed during 2-min sessions. Apexes of ventral and dorsal head excursions were manually measured and used to calculate cycle times. These experiments were repeated with non-Newtonian fluids (3) (dextran; Sigma) with identical results.

Laser Ablation of Neurons. Neurons were ablated as previously described (4), except that worms were immobilized in microbeads. Neuronal classes were identified by expression of fluorophores (GFP or mCherry) with the *dat-1* or *tph-1* promoters (for dopaminergic and serotonergic neurons, respectively). Although fluorophores did not affect behavior when expressed in dopaminergic neurons, expression in serotonergic neurons produced a slight phenotype reminiscent of serotonin-deficient strains (e.g., OH4134, LX959, and three independently derived strains with mCherry). Consequently, all our ablations are compared with shams of the same genetic background, with no phenotypes observed in common with these being reported.

Behavioral Pharmacology. ***Exogenous dopamine.*** Worms in liquid NGM buffer were filmed for 2 min and then transferred to a puddle containing dopamine (25 mg/mL) and filmed for 10 min. Afterward worms were again transferred to NGM puddles, where their recovery was filmed for an additional 10 min.
Exogenous serotonin. Worms were filmed in liquid NGM buffer puddles whose volumes were calibrated to last 10 min (before being absorbed by the underlying agar). Animals were filmed as they exited the vanishing puddles. The experiment was then repeated with puddles containing 5 mg/mL serotonin hydrochloride. Last, the initial experiment was repeated to test for recovery from drug exposure.
Synthesis and use of caged dopamine. Caged dopamine was synthesized as described by Lee et al. (5). Briefly, this involved covalently linking parent compounds to a "caged" moiety (carboxy-2nitrobenzyl). The thus "inactivated" form could be microinjected into different parts of the worms without producing physiological or pharmacological effects until UV illumination broke the covalent bonds.
Bioamine injection. Dopamine, caged dopamine, or control solvent (NGM buffer) was injected using an Olympus IX71 inverted microscope equipped with an IM300 microinjector (Narishige) as previously described (6). Injection concentrations were chosen to yield, upon uncaging, a final concentration in an adult worm as follows: dopamine = 25 mg/mL, serotonin = 8 mg/mL. Injections were performed either immediately posterior to the second pharyngeal bulb (anterior injections) or immediately anterior to the anal pore (posterior injections). Experiments were carried out as described above, after a 15-min recovery period. Worms injected with caged dopamine (or the control NGM) were exposed to unfiltered light from an X-CITE illumination system for 10 s and assayed again.

Optogenetics. Methods were as previously described (7). Briefly, worms were cultured in the dark, on agar plates containing OP50 bacteria and all-trans retinal (Sigma-Aldrich). During experiments, worms were exposed to 1.6 mW/mm^2 blue light produced by an X-CITE illumination system (EXFO) filtered through a GFP excitation filter. Multisite Gateway (Invitrogen) reactions were used to generate *Ptph-1::ChR2::YFP::unc-54UTR* and *Pdat-1::ChR2::YFP::unc-54* UTR vectors (confirmed by sequencing). The strain JPS48 was generated by injection of *Pdat-1::ChR2::YFP::unc-54* construct (300ng/μL) and *Pmyo-3::mCherry::unc-54UTR* (1.5 ng/μL) into WT worms. The strain JPS100 was generated by injection of *Pdat-1::ChR2::YFP::unc-54* construct (300ng/μL) and *Pmyo-3::mCherry::unc-54UTR* (1.5 ng/μL) into RB756 *lite-1*. The *lite-1* mutant was used as a background strain because, unlike WT worms, it does not respond to blue light owing to deletion of a blue-light receptor (8).

1. Avery L, Horvitz HR (1990) Effects of starvation and neuroactive drugs on feeding in *Caenorhabditis elegans*. *J Exp Zool* 253:263–270.
2. Korta J, Clark DA, Gabel CV, Mahadevan L, Samuel ADT (2007) Mechanosensation and mechanical load modulate the locomotory gait of swimming *C. elegans*. *J Exp Biol* 210: 2383–2389.
3. Fang-Yen C, et al. (2010) Biomechanical analysis of gait adaptation in the nematode *Caenorhabditis elegans*. *Proc Natl Acad Sci USA* 107:20323–20328.
4. Bargmann CI, Avery L (1995) *C. elegans: Modern Biological Analysis of an Organism*, eds Epstein HF, Shakes DC (Academic Press, New York), pp 225–250.
5. Lee TH, Gee KR, Ellinwood EH, Seidler FJ (1996) Combining 'caged-dopamine' photolysis with fast-scan cyclic voltammetry to assess dopamine clearance and release autoinhibition in vitro. *J Neurosci Methods* 67:221–231.
6. Mello CC, Kramer JM, Stinchcomb D, Ambros V (1991) Efficient gene transfer in *C. elegans*: Extrachromosomal maintenance and integration of transforming sequences. *EMBO J* 10:3959–3970.
7. Liewald JF, et al. (2008) Optogenetic analysis of synaptic function. *Nat Methods* 5: 895–902.
8. Edwards SL, et al. (2008) A novel molecular solution for ultraviolet light detection in *Caenorhabditis elegans*. *PLoS Biol* 6:e198.

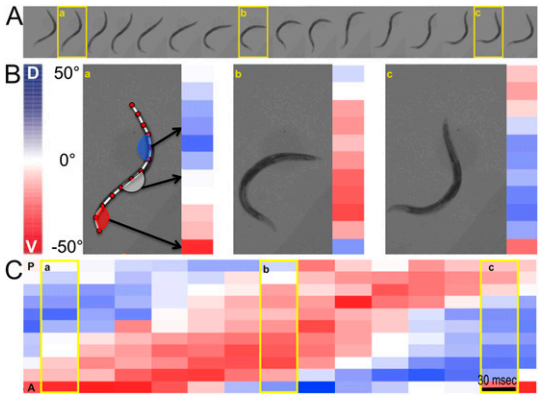

Fig. S1. Example of a single WT swim cycle and how the curvature matrices were constructed. (*A*) Time series of postures made by a single worm. Movies of behaving animals were imported into ImagePro Plus. (*B*) The software extracted the worm from the background and divided its midline into 12 segments of equal lengths. These segments defined 11 angles, which were colored to encode both the direction the animal was bending (red for ventral and blue for dorsal) as well as the amplitude of the motion (conveyed by the brightness of the color). These were used to construct curvature columns that effectively describe the body shape of the animal at any given time. (*C*) Curvature columns were thus assembled into curvature matrices to show how the shape of the animal changed over time during behaviors. In this example, a ventral bend initiated at the head propagates to the tail, as indicated by the upward red. By contrast, fixed postures are indicated by static pattern with the curvature matrix (e.g., Fig. 3*C*). D, dorsal; V, ventral; *P*, posterior; A, anterior.

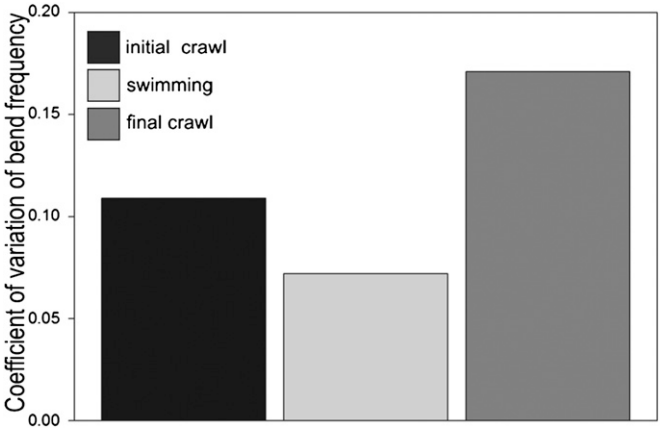

Fig. S2. Crawling frequency is more variable than swimming frequency. Coefficient of variation for WT worms during the three consecutive stages of our behavioral assay shows reduced variability during swimming. Coefficients were calculated as the ratio of the SD.

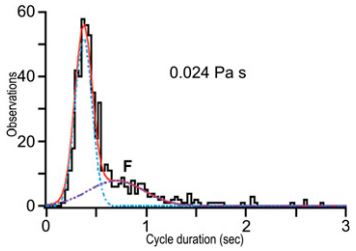

Fig. S3. All-points histogram of cycle durations for *che-3* mutant. Mutant *che-3*, which lacks functional ciliated sensory neurons, displayed swim and crawl-like motion in low-viscosity solution, as evident by a bimodal distribution fit by two Gaussians. Foraging (F) was observed during the slower of the two behaviors.

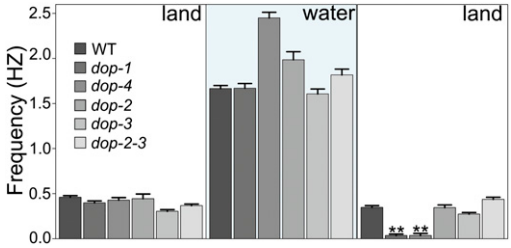

Fig. S4. D1-like dopamine receptors are required for swim-to-crawl transition. Although worms lacking different dopamine receptors could crawl and swim, worms lacking D1-like receptors (*dop-1* or *dop-4*) failed to transition from swimming to crawling, whereas worms lacking D2-like receptors (*dop-2*, *dop-3*, and *dop-2–3*) transitioned normally.

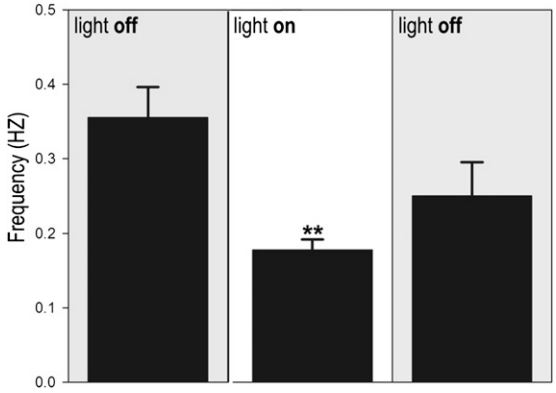

Fig. S5. Light activation of dopaminergic neurons induces basal-slowing in crawling worms. We photostimulated dopaminergic neurons (via *Pdat-1::ChR2*) of crawling WT worms.

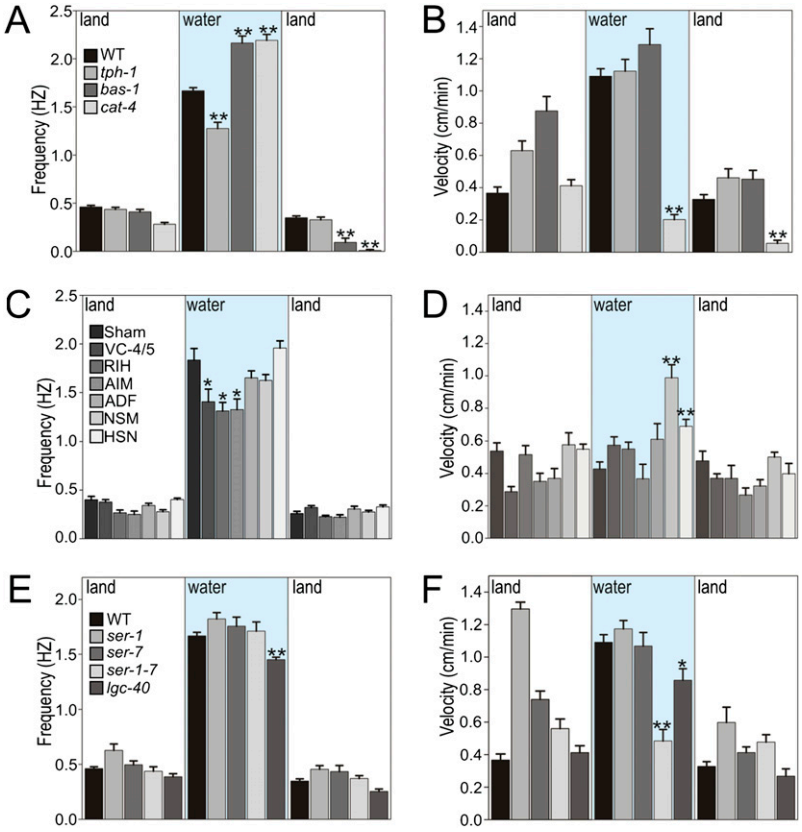

Fig. S6. Serotonergic pathway deficiencies impair swim execution. (*A*) Lack of serotonin synthesis (*tph-1*) but not of both serotonin and dopamine (*cat-4* and *bas-1*) produces swimming impairments that include bouts of crawl-like motion. (*A* and *B*) Note postswim immobilization in worms deficient in dopamine production. (*C*) Ablation of each serotonergic neuronal class showed that animals lacking VC-4, -5, RIH, or AIM neurons had deficient swimming with bouts of crawl-like motion. (*D*) Ablation of NSM increased swimming (but not crawling) velocity. (*E*) Worms lacking the serotonin-gated ion channel LGC-40 showed impaired swimming performance with bouts of crawl-like motion. (*F*) Additionally, both LGC-40 and worms lacking the G protein-coupled serotonin receptors SER-1 and SER-7 had impaired swimming velocities.

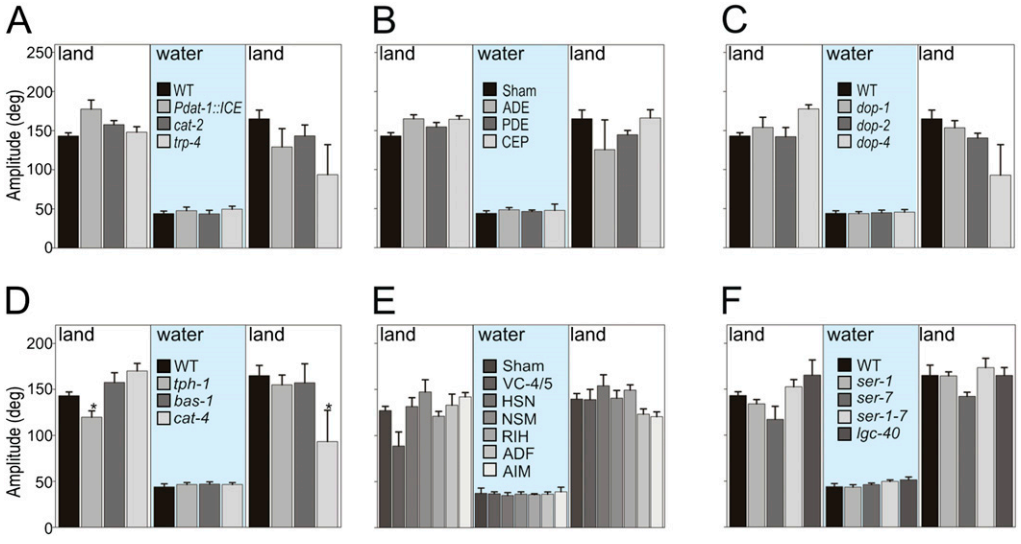

Fig. S7. Angular excursion of the neck for worms with impaired dopaminergic and serotonergic pathways. Deficiencies in dopaminergic pathways seen in worms defective in dopamine production (*A*), ablated dopaminergic neurons (*B*), or deficient in dopamine reception (*C*) did not affect the amplitude of neck movement compared with controls. The larger SEM observed for the postswim crawls are associated with partial or incomplete neck waves seen in immobilized animals. Deficiencies in aminergic pathways as demonstrated by worms defective in serotonin production (*D*), ablated serotonergic neurons (*E*), or deficient in serotonin reception (*F*) did not affect the amplitude of neck movement compared with controls. The postswim effect observed for *cat-4* mutants (*D*) was associated with postswim immobilization and can be understood in the light of this gene's role not only in serotonin production but also in the synthesis of dopamine.

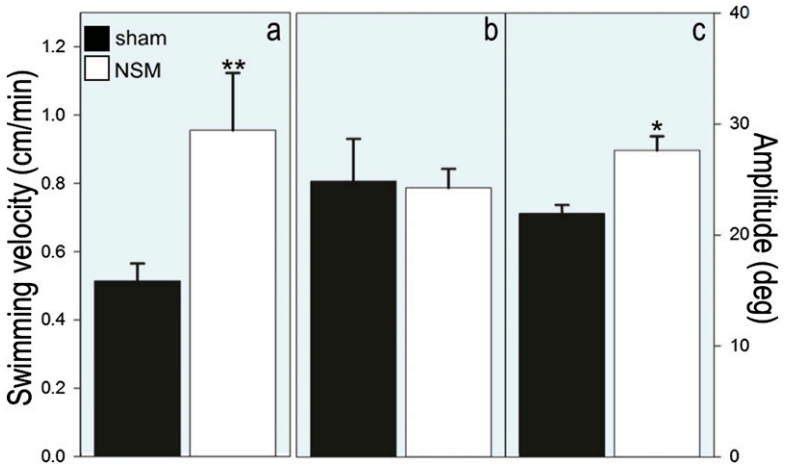

Fig. S8. (*A*) Ablation of the NSM serotonergic neurons resulted in increased swimming velocity. (*B*) This velocity was observed despite a decreased swimming frequency (Fig. S6*C*) and unaffected neck angular excursions (Fig. S7*E*). (*C*) Swimming velocity however is accompanied by an increase in tail excursion angles.

Movie S1. Behavioral assay to study transitions between crawling and swimming performed by a typical WT worm. A representative, individual adult worm was placed on a smooth agar plate and allowed to acclimate for 2 min. After this time it was filmed at 30 fps as it crawled and entered a 3-μL puddle of water. After approximately 5 s the worm began swimming. The worm continued to swim (unable to exit the puddle) while the water was slowly absorbed by the agar substrate. Once the puddle height decreased to the width of the worm, the worm was able to move across the agar surface while dragging the puddle. The worm resumed crawling after all water had vanished. We performed this assay on all of the worms used in this study.

Movie S1

Movie S2. Worms moving in liquids of increasing viscosities. We filmed worms swimming in liquids with increasing methylcellulose concentrations. WT worms immersed in low-viscosity liquids (0.024 Pa s, 0.5% MC) swam. Worms in intermediate viscosities (10 Pa s, 2.3% MC) alternated between swimming and crawling bouts, whereas worms in higher viscosities (50 Pa s, 3% MC) spent most time engaged in crawling behavior. In every case, foraging was observed when worms engaged in the slower of the two behaviors.

Movie S2

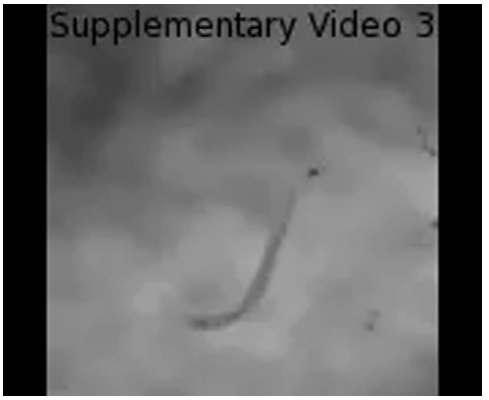

Movie S3. Worms that are fed iron particles swim in water but transition to crawling when specific portions of their body are pulled to substrate by an electromagnet. We fed WT worms a mixture of bacteria (OP50) and small iron particles. We transferred worms to a puddle on an agar-coated slide sitting on top of a custom-built electromagnet. Worms with iron in their bodies could swim normally until the electromagnet was activated. At this point worms with enough particles localized to either the center of their bodies, their heads, or their tails were pinned to the substrate at these areas but remained swimming in place nonetheless. However, when the iron particles were distributed both posterior to the pharynx and in the tail, worms transitioned to crawling until the magnet was deactivated.

Movie S3

Movie S4. Worms lacking dopaminergic neurons fail to transition from swimming to crawling. A worm lacking all dopaminergic neurons (*Pdat-1::ICE*) is able to crawl on smooth agar exposed to air, enter a puddle, and initiate and maintain swimming. After the puddle is absorbed by the water, however, the worm fails to initiate and maintain crawling once again and remains immobile for several to tens of minutes.

Movie S4

Movie S5. Swimming worms expressing Channelrhodopsin-2 in their dopaminergic neurons transition to crawling upon photostimulation. We expressed Channelrhodopsin-2 in dopamine neurons using the *dat-1* promoter. These worms crawled and swam normally but transitioned to a crawl-like motion while in water when their dopaminergic neurons were photostimulated with blue light. The effect was reversible and accompanied by foraging and pharyngeal pumping.

Movie S5

Movie S6. Serotonergic signaling is necessary for proper swim execution and inhibition of crawl-associated behaviors. Worms lacking the G protein-coupled serotonin receptor SER-5 show impaired swimming and inappropriate foraging in water. Worms with deficiencies in their serotonergic signaling pathways had delays in swim onset, impaired swim execution, and inappropriately foraged while swimming.

Movie S6

Movie S7. Exogenous serotonin delays crawl onset. We measured the time elapsed from the moment the puddle had receded enough to produce a noticeable meniscus around the worm's body (and thus imply continuous firm contact between the worm and the substrate) and the time when the worm finished crossing the outline of the original puddle (*A*). We found that WT worms swimming in low concentrations of exogenous serotonin (5mg/mL) continued to swim as the puddle receded and delayed crawl onset (*B*).

Movie S7

Movie S8. Crawling worms expressing Channelrhodopsin-2 in their serotonergic neurons show increased bend frequency on land upon photostimulation. We expressed Channelrhodopsin-2 in serotonergic neurons using the *tph-1* promoter. Photostimulation of serotonergic neurons significantly increased crawl frequency on land.

Movie S8